Proximal tubule-on-chip as a model for predicting cation transport and drug transporter dynamics

Isy Petit, Quentin Faucher, Jean-Sébastien Bernard, Perrine Giunchi, Antoine Humeau, François-Ludovic Sauvage, Pierre Marquet, Nicolas Védrenne, Florent Di Meo

scientific reports

Check for updates

OPEN

Proximal tubule-on-chip as a model for predicting cation transport and drug transporter dynamics

Isy Petit[1], Quentin Faucher[2], Jean-Sébastien Bernard[1], Perrine Giunchi[1,3,4], Antoine Humeau[1], François-Ludovic Sauvage[1], Pierre Marquet[1,5], Nicolas Védrenne[1,7]✉ & Florent Di Meo[1,6,7]✉

Deciphering the sources of variability in drug responses requires to understand the processes modulating drug pharmacokinetics. However, pharmacological research suffers from poor reproducibility across clinical, animal, and experimental models. Predictivity can be improved by using Organs-on-Chips, which are more physiological, human-oriented, micro-engineered devices that include microfluidics. OoC are particularly relevant at the fundamental and preclinical stages of drug development by providing more accurate assessment of key pharmacokinetic events. We have developed a proximal tubule-on-a-chip model combining commercial microfluidic and chip technologies. Using the RPTEC/TERT1 cell line, we set up a dual-flow system with antiparallel flows to mimic the dynamics of blood and urine. We assessed transporters mRNA expression, cellular polarization and protein expression via immunofluorescence, and monitored the transcellular transport of prototypic xenobiotics by determining their efflux ratios. Our results show that flow exposure significantly modulate mRNA expression of drug membrane transporters. Dynamic conditions also enhance cell polarization, as evidenced by preferential basal and apical expressions of Na + /K + -ATPase, P-gp, OCT2, and MATE1 , as well as the cellular secretory profile. We demonstrated unidirectional transcellular transport of metformin with a higher efflux than influx ratio, inhibited with OCT2 inhibitor, thus confirming the relevance of our proximal tubule-on-a-chip set up for cation transport investigations. Our proximal tubule-on-a-chip can also be used to explore the interactions between transporters, xenobiotics, and endogenous metabolites, possibly involved in the variability of individual drug responses. This study provides additional evidence that OoC can help bridge the gaps between systemic and local pharmacokinetics.

Keywords Organ-On-a-Chip, Pharmacokinetics, Drug membrane transporters, Proximal tubule-On-a-Chip, Drug-Drug Interactions, Drug-Endogenous metabolite Interactions

Abbreviations

ABC	ATP-Binding Cassette
ATCC	American Type Culture Collection
DDI	Drug-Drug Interactions
DMI	Drug-Endogenous Metabolite Interactions
FSS	Flow Shear Stress
ITC	International Transporter Consortium
MATE	Multidrug and Toxin extrusion protein
OAT	Organic Anion Transporter
OCT	Organic Cation Transporter
OoC	Organ-on-chip
P-gp	P-glycoprotein

[1]U1248 Pharmacology & Transplantation, Inserm, Univ. Limoges, Limoges, France. [2]Division of Pharmacology, Utrecht Institute for Pharmaceutical Sciences, Utrecht University, Utrecht, the Netherlands. [3]Institut de Recherche en Santé Digestive, INSERM, INRAE, ENVT, Univ. Toulouse III, Toulouse, France. [4]Institut de Mécanique Des Fluides de Toulouse (IMFT), CNRS, Univ. Toulouse, Toulouse, France. [5]Department of Pharmacology, Toxicology and Pharmacovigilance, CHU Limoges, Limoges, France. [6]UAR2015/US42 Integrative Biology Health Chemistry and Environment BISCEm, CNRS, Inserm, CHU Limoges, Univ. Limoges, Limoges, France. [7]Nicolas Védrenne and Florent Di Meo are contributed equally. ✉email: nicolas.vedrenne@unilim.fr; florent.di-meo@inserm.fr

PK	Pharmacokinetics
PT	Proximal Tubule
RPTEC	Renal Proximal Tubule Epithelial Cell
RSS	Remote Sensing Signaling
SLC	Solute Carrier

The inherent limitations of preclinical models drastically underestimate the high complexity of the human body, leading to discrepancies between observations obtained at different stages (clinical, in vivo, in vitro and in silico). Over the past decades, substantial efforts have been carried out to unravel pharmacological events governing xenobiotic concentrations (pharmacokinetics, PK) either locally or systematically[1,2]. In this context, drug transporters expressed at the intestinal, hepatic, renal, blood–brain and renal barriers, including the Solute Carrier (SLC) and ATP-binding cassette (ABC) families, are particularly relevant. These membrane proteins facilitate the transport of endogenous metabolites as well as xenobiotics from one compartment to another across epithelial barriers. Those expressed in the kidney proximal tubule (PT) play an important role in drug disposition. Since 2010, The International Transporter Consortium (ITC) has identified several drug membrane transporters of clinical importance that should or must be investigated not only in drug development but also retrospectively, after drug approval if not done before[3–7]. This list includes SLCs, namely organic anion transporters (*SLC22A6*/OAT1 and *SLC22A8*/OAT3), organic cation transporter 2 (*SLC22A2*/OCT2) and multidrug and toxin extrusion proteins (*SLC47A1*/MATE1 and *SLC47A2*/MATE2-K) as well as ABC transporters such as P-glycoprotein (*ABCB1*/P-gp). Importantly, these transporters are also cited by regulatory agencies (*e.g.*, the Food and Drug Administration and the European Medicines Agency) in their guidance documents for drug development, with a particular focus on drug-drug interactions (DDI). Noteworthy, retrospective investigations on multidrug resistance associated proteins (*ABCC2*/MRP2 and *ABCC4*/MRP4) are also recommended by ITC to elucidate their potential involvement in drug disposition from clinical observations[7].

These PT transporters also participate in maintaining endogenous metabolite homeostasis[8,9]. Their physiological-pharmacological duality is now leveraged by the Remote Sensing and Signaling (RSS) Theory that relies on the presence of multi-specific and oligo-specific transporters in different organs that form a multi-scale, adaptive communication network that maintain or restore endogenous metabolite homeostasis[10]. One can easily hypothesize that drugs and their metabolites modulate the so-called RSS network via membrane transporters. Likewise, endogenous metabolite might influence local drug PK by affecting their intracellular and tissue concentrations. Such transporter-mediated drug-endogenous metabolite interactions (DMI) can represent a source of PK variability yet poorly explored, and dysregulate endogenous metabolism leading to off-target pharmacodynamics effects, locally as well as at distant sites.

Conventional models are not suited to study these interactions. On the one hand, differences between murine and human membrane transporters can lead to poor prediction of DDI and DMI[11,12]. On the other hand, conventional static 2D in vitro cell models do not sufficiently recapitulate the physiological or pathological mechanisms occurring *in situ*[13]. However, the last decade has seen the advent of new in vitro models called "microphysiological systems" , defined as devices or culture methods aimed at improving the physiological response of cells in experimental models. Organs-on-chips (OoCs) are defined as cell culture devices and methods that include a microfluidic-controlled microenvironment [14,15]. These systems recreate physiological flows in the target organ, such as urine and blood flow in the case of renal PT. The flow is perceived by cells thanks to mechanosensory mechanisms[16], including primary cilia, which in turn favor cell polarization, protein expression and metabolic functions[17–20]. One of the main challenges of OoC is achieving reproducibility, and another is standardization of protocols across laboratories[21,22]. The sources of variability are many, including the flow system setup, tubing length and diameter, chip geometry (often homemade), flow rate, exposure time, etc. Only a few teams provided detailed descriptions of their operating modes. Most published kidneys-on-chips used proximal tubule cells, as this part of the nephron is the main kidney site for drug reabsorption, secretion[23] and a critical target for drug-induced nephrotoxicity[24–26]. The most commonly used kidney-on-chip configuration is an applied mono flow on tubular epithelial cells culture on 2D[26]. Additionally, only a few groups have studied the unidirectional transcellular transport of xenobiotics, and/or DDI and DMI. Noteworthy, Ma et *al.* have recently proposed a PT-on-chip based on induced human stem cells and a homemade device for functional investigations of renal transporters[27]. However, such models are challenging to scale up for drug screening due to their complexity (cellular heterogeneity and lack of maturation), moreover most do not use commercial devices but custom-made chips.

The present study aimed to develop a PT-on-chip model for the purpose of investigating DDI and DMI as a potential source of local PK variability, as the first step towards the development of a platform encompassing several key pharmacological organs for systemic pharmacology purposes. It relies on the use of commercially available immortalized RPTEC/TERT1 cell lines, micro-perfusion system and chips. Given the well-known poor expression of OAT transporters in RPTEC/TERT1 cells[28,29], we focused on the interplay between cationic probes and the OCT2/MATEs-driven transcellular transport, accounting for DDI and DMI. Using metformin and creatinine as pharmacological and endogenous probes respectively, we confirmed our PT-on-chip is functional and, has pharmacological relevance. Transporter-mediated DDI or DMI through the unidirectional OCT2/MATE transcellular transport were further explored considering transport inhibitors.

Materials and methods

Cell culture

RPTEC/TERT1 were obtained from American Type Culture Collection (ATCC) (ATCC, reference: CRL-4031), and cultured in Dulbecco's modified Eagle's medium with Ham's F-12 nutrient mix (DMEM: F12) (ATCC, reference: 30–2006) supplemented with hTERT immortalized RPTEC Growth kit (ATCC, reference: ACS-4007),

penicillin/streptomycin (Gibco, reference: 15,140,122) at 1% and Geneticin (Gibco, reference: 10,131,035) at 0.2%. No FBS was used. Cells were cultured routinely in T75 flasks (Sarstedt, TC Flask T75, Cell+, Vented Cap, reference: 83.3911.302) at 37 °C in a 5% CO2 humidified atmosphere. Cells were sub cultured by trypsinization with 0.25% trypsin (Gibco, reference: 25,200,056), and the media was changed every two days. The cells used for further experiments were at passages 4 to 15.

Microfluidics setup

The Elveflow OB1 MK4 microfluidic system from Elveflow (Paris, France) (Figure S1) includes a pressure- and flow-controller that apply pressure on a reservoir connected to a microfluidic flow sensor. It adapts the pressure to maintain the user-defined flow rate. A recirculation pump was added to the system to limit media consumption and prolong the contact time between cells and fluids. The tubing setups (lengths, diameter) are reported in Figure S1.

Proximal tubule-on-a-chip

RPTEC/TERT1 were seeded at 130 000 cells/cm^2 on µ-slide I luer ibitreat chips (ibidi, Cat. No: 80176) or on Be-doubleflow standard chips (Beonchip), depending on the experiment. All supports were thin coated with collagen 1 (Gibco, reference: A1048301) at 5 µg/cm^2 according to the manufacturer's protocol. µ-Slide I luer ibitreat consists in one channel of 50 mm length, 5 mm width and 0.4 mm height. Be-doubleflow chip consists in 2 channels of 46 mm length, 1.5 mm width and 0.375 mm height. Channels are separated by a semi-porous membrane with a random distribution of pores across an average diameter of 1 µm. Six hours after seeding, cell cultures on chips were placed on a cell culture rocker with a 5% angle. Cells were cultured for 10 days at 37 °C in a 5% CO_2 humidified atmosphere, and the culture medium was changed every day.

Quantification of mRNA transcripts

NucleoSpin RNA (Macherey–nagel, reference: 740,955.250) or NucleoSpin RNA XS (Macherey–nagel, reference: 740,902.50) kits was used to extract mRNA, according to the manufacturer's protocols. Extract were then stored at -80 °C until analysis. After quantification and integrity evaluation, complementary DNA was obtained using the Master Mix SuperScript™ IV VILO™ (reference:11,756,050), according to the manufacturer's protocol. Gene-specific primer–probe (table S1) sets and Master Mix TaqMan™ Fast Advanced, no UNG (reference: A44360) was purchased from ThermoFisher scientific. Quantitative PCR (qPCR) reactions were carried out in duplicate with 25 ng of DNA with the Rotor-Gene Q 2plex from QIAGEN and the Rotor-Gene Q Series Software (version 2.3.5 – Build 1, https://www.qiagen.com/us). Gene expression levels were normalized to GAPDH expression and expressed as fold-difference compared to the control.

Immunofluorescent cell staining for confocal imaging

For immunofluorescent staining, cells were fixed with 1% PFA for 10 min at room temperature. After 3 steps of washing with phosphate-buffered saline (PBS, Gibco, reference: 14,190–094), the non-specific sites were saturated with 3% PBS-Bovine serum albumin (BSA, Sigma, reference: A9418-10G) for 1 h. After washing steps with PBS, the chips were spiked with a primary antibody diluted with PBS-BSA 3% for 12 h at 4 °C. After another 3 PBS washing steps, chips were treated with a solution of secondary antibodies (Table S2) for 1 h at room temperature. After PBS washing, chips were spiked with DAPI (Invitrogen, reference: D1821) at [300 nM] for 5 min. After PBS washing, the chips were spiked with the CitiFluor™ AF1 mountant solution (Electron microscopy sciences, cat. N° 17,970.25) before confocal imaging with ZEISS LSM880.

Polarized transport study

Transporter activity assay

RPTEC/TERT1 were seeded on the apical channel of BE double flow chip, and cultured as described previously, after ten days they were put under antiparallel flows at 10 µL/min (or 0.03 dyn/cm^2) for the apical channel to model urine flow and 20 µL/min (0.07 dyn/cm^2) for the basal channel to model blood flow (Figure S1). After 24 h under flow transcellular transport through the PT epithelial barrier was evaluated by measuring the apparent permeability for metformin [100 µM] (M), creatinine [10 µM] (C) or tenofovir [30 µM] (T) at the apical (A) or basal (B) sides, for A-to-B or B-to-A permeability assessment 24 h later. Permeability was also measured after transport inhibition with, cimetidine [100 µM], ritonavir [15 µM] and diclofenac [30 µM]. Circulating fluids were collected at the beginning (T_0) and after 24 h of substrate exposure. Apparent permeabilities were measured under both the rocker-based perfusion on a cell culture rocker or under flow shear stress (FSS) conditions.

Compound quantitation by LC–MS/MS

The extraction of extracellular metabolites was performed as already described in Faucher et *al*[30]. The cell culture medium was collected and centrifuged at 3000 g for 1 min at room temperature to eliminate cell debris. Then 200 µL of acetonitrile and 20 µL of internal standard solution (2-isopropylmalic acid, 0.5 mM) were added to 100 µL of supernatant. Solutions were homogenized by vortex mixing for 30 s and centrifuged at 15,000 g for 15 min at room temperature. Solutions were diluted 1/10 with ultrapure water and transferred into an injection vial for mass spectrometry analysis. Three microliters of the extracts were injected into the LCMS-8060 (Shimadzu, Kyoto, Japan) liquid chromatography—tandem mass spectrometry system. Metformin, tenofovir and creatinine concentrations were measured against a calibration range.

Efflux ratio calculation

The concentration obtained by mass spectrometry were used to calculate the efflux ratio, as follows:

$$\text{Efflux Ratio} = \frac{P_{app}(B \text{ to } A)}{P_{app}(A \text{ to } B)}$$

where P_{app} is the apparent permeability coefficient (cm/s) calculated for each compound for the apical-to-basolateral (A to B) and basolateral-to-apical (B to A) directed transport:

$$P_{app} = \frac{dQ}{dt} \times \frac{1}{S \times C_0}$$

where $\frac{dQ}{dt}$ is the rate of drug appearance in the receiver compartment (mol/s), S is the surface area of the membrane (cm^2), C_0 is the initial concentration of the drug in the donor compartment (mol/cm3).

Metabolomics study

Extracellular metabolites were extracted from the cell culture medium as described in Sect. "Compound quantitation by LC-MS/MS". three milliliters of the extracts were injected into the same analytical system as above, using the LC–MS/MS "Method Package for Cell Culture Profiling Ver.2" (Shimadzu) where mass transitions of additional compounds had been added locally by infusing the pure substances in the mass spectrometer. For each transition analyzed, only well-defined chromatographic peaks were considered setting up the signal-to-noise ratio threshold at 10. The area under the curve of each metabolite was normalized to the area under the curve of the internal standard (2-isopropylmalic acid).

Statistical analysis

One-way analyses of variance (ANOVA) with Dunnett multiple comparison tests, or Kruskal–Wallis tests were performed using GraphPad Prism (version 10.1.1, GraphPad Software Inc., San Diego, CA, USA, https://www.graphpad.com/). All data in figure and text are presented as means + /- standard deviation; differences between groups were considered statistically significant for $p < 0.05$. All the RT qPCR statistical data are presented in Table S3.

AI-assisted technologies in the writing process

During the preparation of this manuscript, we used ChatGPT 3.5 in order to check grammar and spelling as well as to improve readability of the manuscript. After using this tool, we reviewed and edited the content as needed. Thus, we take full responsibility for the content of the present manuscript.

Results

Impact of flow exposure on cell transporter expression and metabolome

mRNA expression of drug membrane transporters

Given the inherent challenges regarding reproducibility and harmonization across OoC setups, the RPTEC-TERT1 cell culture protocol was first optimized as described in Fig. 1A. The best compromise between cell viability, monolayer architecture and transporter expressions was achieved by: (i) seeding at 130 000 cells/cm^2; (ii) exposing post-confluence monocellular layers to rocker-based perfusion for 9 days using a rocker (5° inclination, 1 cycle per minute); and (iii) finally applying predefined FSS for 4 days. In the present section, we employed commercial mono-channel chips to investigate the effects of flow.

Different flow rates (5, 10 and 20 µL/min *i.e.*, 0.0045, 0.009 and 0.02 dyn/cm^2, respectively) were first considered to assess the mRNA expression of drug membrane transporters of pharmacological relevance. Particular attention was paid to *ABCB1*, *ABCC2*, *ABCC4*, *ABCG2* (see Fig. 1B) and *SLC22A2*, *SLC22A4*, *SLC22A5*, *SLC47A1* and *SLC47A2* (see Fig. 1C). Controlled flow exposure was associated with increased mRNA expression of ABC transporters. The higher the flow rate, the higher the mRNA expression of *ABCB1*, *ABCC2* and *ABCC4*. By contrast, *ABCG2* gene expression was only significantly increased at 5 µL/min ($p = 0.027$) at 20 µL/min ($p = 0.003$), but not at the intermediate 10 µL/min flow rate. Shear stress also increased the transcriptomic expression of SLC transporters, except for *SLC22A4* and *SLC22A5*, for which mRNA expression was either unchanged (*SLC22A4*) or decreased (*SLC22A5*, see Fig. 1C). *SLC47A1* and *SLC47A2* were significantly increased at 5 µL/min for SLC47A1 ($p = 0.037$) and at 10 µL/min for SLC47A1 ($p = 0.005$) and SLC47A2 ($p = 0.002$). However, they are more sensitive to shear stress than *SLC22A2*. SLC transporters mRNA expression was not correlated with the flow rate. Additionally, mRNAs of *SLC22A6* nor *SLC22A8* were not detected under rocker-based perfusion or FSS conditions, as expected with RPTEC/TERT1 cell lines[28,29]. Means, SD and SEM for all transporters and conditions are reported in Table S3.

Cell secretory profiles under flow conditions

Likewise, the cell excreted secretome was compared between rocker-based perfusion and FSS conditions on commercial mono-channel chips, by monitoring metabolite concentrations in the medium. Serum-free conditions were used to ensure that the metabolites identified were not artefactual. More than 103 metabolites were searched (Table S4), of which only 33 were detected (Table S5). Interestingly, two different behaviours were observed: 13 metabolites exhibited increased concentrations and 17 decreased concentrations under flow conditions, as compared to the rocker-based perfusion conditions (Fig. 1D). Even though these modifications are mild, they highlight that shear stress modulates intracellular metabolisms and cellular absorption/secretion behaviors. Metabolic profiles did not exhibit a flow rate/concentration relationship likely due to experimental

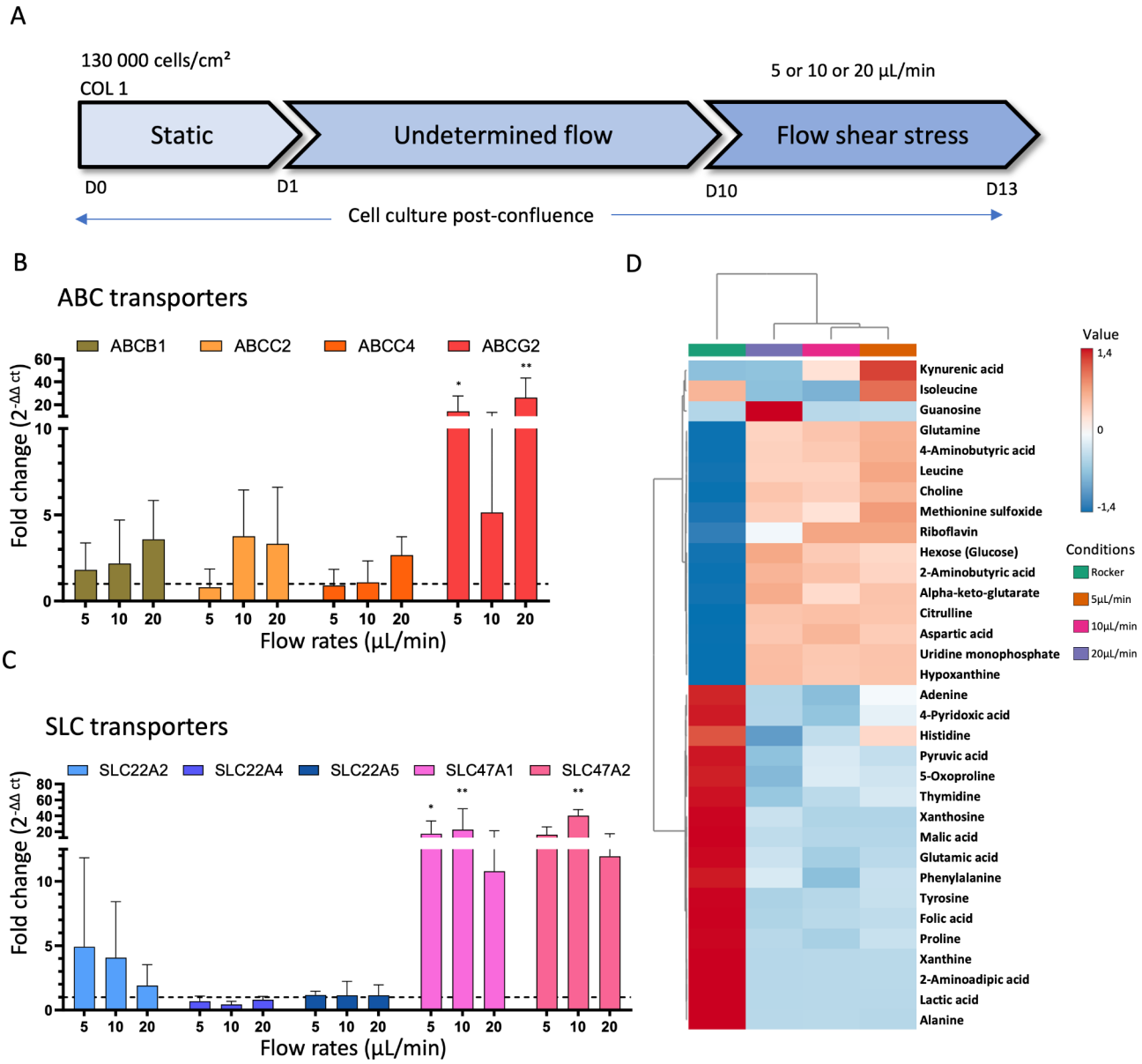

Fig. 1. Flow shear stress influences drug transporter transcriptomic expression and endogenous metabolite production. (**A**) Protocol used for RPTEC/TERT1 cell culture in proximal tubule-on-chip in the present study. (**B**-**C**) Fold changes regarding the mRNA expressions of proximal tubule ABC and SLC transporters of pharmacological relevance. Bar plots show relative expression levels of RPTEC/TERT1 mRNA transporter expressions using mono-channel device where cells are exposed to different flow rates, 5 µL/min (0,0045 dyn/cm^2, N = 6), 10 µL/min (0,009 dyn/cm^2, N = 11) and 20 µL/min (0,02 dyn/cm^2, N = 4). It is worth mentioning that for *SLC22A4*, *SLC22A5* and *SLC47A2*, only three independent replicas (N = 3) were performed. Expression levels were normalized to the internal control GAPDH gene and are presented as fold changes relative to rocker-based perfusion conditions (N = 5, dotted line). Error bars represent standard deviations. Statistical significances were conducted using one-way ANOVA analysis, asterisks (*) indicate statistically significant differences compared to rocker-based perfusion condition (*p-value < 0.05, **p-value < 0.01, ***p-value < 0.001). (D) Targeted search for 33 endogenous metabolites out of 103 initially considered (see main text) by LC–MS/MS on extracellular supernatant of RPTEC/TERT1 cells culture in rocker-based perfusion (Rocker) condition or exposed to different flow rates (5, 10 and 20 µL/min). Data were standardized by auto scaling and hierarchically clustered with Ward method and represented by mean of 3 independent replicates. Metabolomic clustering was achieved using the MetaboAnalyst 6.0 Statistical Analysis online tool.

conditions, except for kynurenate and isoleucine. Thereby, no specific pathway can be identified, requiring further investigations which are beyond the scope of the present study.

Cell polarization and architecture

An epithelial barrier suited to model PT elimination function requires proper cell polarization, which is not often checked in conventional static 2D culture models[20]. We investigated cell polarization under dynamic conditions by monitoring protein expression and localization using immunofluorescence. We first focused on P-gp and Na + /K + -ATPase protein expression, indicating proper basal to apical polarization (Fig. 2A). They were mostly expressed at the basal and apical membrane, respectively, as evidenced by z-stack analyses using

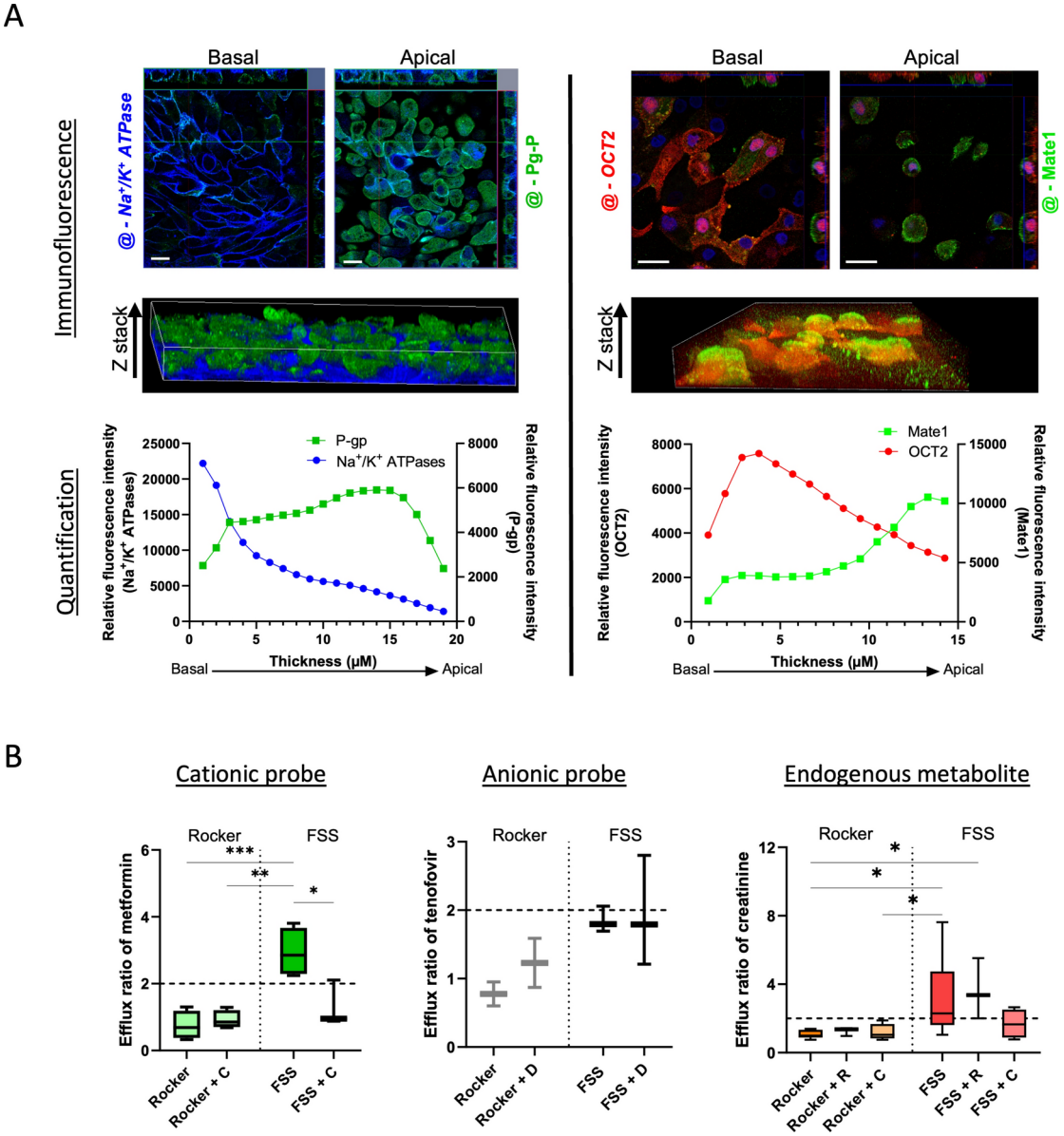

Fig. 2. Expression, localization and function of specific transporter under flow conditions. (**A**) Apical and basal immunostaining of Na^+/K^+ ATPase (left panel, blue), P-gp (left panel, green), OCT2 (right panel, red) and, MATE1 (right panel, green) conducted on RPTEC/TERT1 cell line in mono channel device under FSS (20µL/min, i.e., 0,02 dyn/cm^2) as well as 3D reconstruction and quantification of relative fluorescent intensity along cell layer thickness. (**B**) Calculated efflux ratios of metformin (left), tenofovir (center) and creatinine (right) under rocker-based perfusion (Rocker) and FSS. Experiments were either conducted with standalone substrate (metformin, 100 µM, N = 4; tenofovir, 30 µM, N = 3; creatinine, 10µM, N = 8) or in presence of inhibitor (metformin/cimetidine (**C**), 100µM/100µM, N = 3; creatinine/cimetidine, 10µM /100µM, N = 4; creatinine/ritonavir (R), 10 mM/15 mM, N = 3; and tenofovir/diclofenac (**D**), 30µM/30µM, N = 4). Statistical significance was determined using one-way ANOVA, asterisks (*) indicate statistically significant differences compared with rocker-based perfusion (*p-value < 0.05, **p-value < 0.01, ***p-value < 0.001).

confocal microscopy. Likewise, but to a lesser extent, OCT2 and MATE1 protein were also expressed at proper location, at the basal and apical membrane respectively (Fig. 2A). Interestingly, immunofluorescence also indicated intracellular expressions of membrane transporters, but not Na+/K+-ATPase. Importantly, OAT1 was not observed by immunofluorescence, as expected from (i) the literature and (ii) their mRNA expression levels (see above). OAT3 was observed using immunostaining under the rocker-based perfusion and FSS conditions (Figure S2).

Modeling xenobiotic elimination using PT-on-chip

Transporter-mediated transcellular transport of pharmacological probes

Transporter-mediated transcellular transport was then investigated to ensure that the PT-on-chip setup developed reliably model one of the main pharmacological functions of PT epithelial cells, i.e., elimination of xenobiotics and metabolites from blood into urine. We check the relevance of dual channel chips as compared to mono channel devices by measuring mRNA expression of membrane transporters (Figure S3). The epithelial barrier integrity was assessed by monitoring Dextran-FITC transport from the apical to the basal channel (Figure S4) where no impact of metformin treatment was detected.

We measured apparent permeabilities of metformin and creatinine, known substrates for the basal–apical OCT2-MATE transporter pair. We also perform assay for tenofovir as a negative control, since it is transported by OAT1/3 and MRP2/MRP4 at the basal and apical membranes, respectively (Figure S5). Interestingly, apparent permeabilities under FSS conditions are one order of magnitude lower than under rocker-based perfusion conditions owing to the higher flow rate associated with lower substrate residence time due to velocity. Efflux ratios were then calculated to measure the unidirectional (or vectorial) transcellular transport. For the OCT2/MATEs transporter pair, the vectorial transports under FSS were significantly higher for metformin (efflux ratio: 2.94 ± 0.727, $p < 0.001$) and creatinine (3.24 ± 2.21, $p = 0.01$) (Fig. 2B), than under rocker-based perfusion, where no vectorial transcellular transport was observed for metformin (0.75 ± 0.42) and creatinine (1.06 ± 0.23).

As expected, our PT-on-chip setup does not properly express vectorial transport involving OATs/MRPs pairs (tenofovir efflux ratio: 1.85 ± 0.19 and 0.78 ± 0.25 under the FSS and rocker-based perfusion conditions, respectively), due to insufficient expression of influx OATs at the RPTEC/TERT basal membrane.

Modeling transporter-mediated drug-drug and drug-metabolite interactions

We used cimetidine, a known OCT2/MATEs inhibitor, to investigate the pharmacological relevance of the present PT-on-chip model further. Under rocker-based perfusion conditions, cimetidine did not influence metformin (exogenous substrate) (efflux ratios: 0.92 ± 0.27) and creatinine (1.18 ± 0.43) (endogenous substrate) transport (Fig. 2B). In contrast, under FSS it decreased metformin (1.31 ± 0.69, $p = 0.016$) and creatinine efflux (1.68 ± 0.85), supporting the inhibitory effect of cimetidine on either OCT2 or MATE1/MATE2K transporters. Creatinine efflux ratio was not significantly inhibited by ritonavir, a known inhibitor of OCT2 but not MATE (3.63 ± 1.77), suggesting a higher affinity of creatinine to OCT2 than ritonavir.

For the sake of comparison, an OAT inhibitor (diclofenac) was also associated with tenofovir, showing no effect on its efflux ratio (1.93 ± 0.81), but the latter was already below the threshold of 2 without inhibitor.

Modulating transporter expressions and secretome by transporter substrates

Under FSS, PT transporter expression and intracellular metabolism were investigated after xenobiotic or creatinine exposure. In the presence of metformin, transcriptomic analyses revealed an upward trend for mRNA expression of ABC and SLC transporters (significant for *ABCC2* ($p = 0.007$), *ABCC4* ($p = 0.028$), *SLC47A1* ($p = 0.012$), *SLC47A2* ($p = 0.007$) and *SLC22A5* ($p = 0.007$)), except for *ABCG2* (Fig. 3A). Interestingly, when cimetidine was added, mRNA expression increases were all abolished, except for *SLC47A1* whose mRNA expression was slightly, although not significantly, increased as compared to the control. In contrast, when PT-on-chip was exposed to creatinine, mRNA expression of most membrane transporters remained unchanged, whereas *ABCB1* ($p = 0.015$), *SLC47A1* ($p = 0.032$), *SLC47A2* ($p = 0.035$) were significantly increased (Fig. 3B). Adding ritonavir or cimetidine had no strong impact, except for *ABCC2 (*with cimetidine $p = 0.044$; with ritonavir $p = 0.023$) and *ABCC4 (*with cimetidine $p = 0.021$) where an increase in expression was observed. Means, SD and SEM for all transporter, and condition are reported in table S3. Intracellular metabolism was next evaluated under transporter substrate exposure and compared with the initial conditions T_0 (Fig. 3C). We identified 38 differentially expressed metabolites (Table S6). Five of them were up-regulated and 26 down-regulated by metformin. Creatinine exposure was associated with 12 and 18 up- and down-regulated metabolites, respectively (Fig. 3D). Folic acid and methionine sulfoxide were modulated by both creatinine and metformin, while 13 other metabolites were down-regulated.

Discussion

We developed a functional PT-on-chip set-up that models the transporter-mediated transcellular transport of cationic substrates, whether endogenous or exogenous. This was achieved by using double-flow chip in which different FSS were applied in basal and apical channels. We demonstrated the FSS-dependent mRNA expressions of several membrane transporters namely ABCB1, ABCC2, ABCC4, ABCG2, SLC22A2, SLC47A1 and, SLC47A2 in human immortalized RPTEC/TERT1 cells. Furthermore, the present results show that our PT-on-chip setup with commercial chips recapitulates only under FSS conditions: (i) the unidirectional (or vectorial) transcellular transport of xenobiotics and endogenous metabolites through OCT2, MATE1 and MATE2-K transporters; and (ii) transporter-mediated drug-drug or drug-metabolite interactions. Unfortunately, the present system cannot be used to model unidirectional transcellular transport involving OATs since they are not expressed by the RPTEC/TERT1 cell line, as described in the literature[31,32]. Overexpressing OATs or using commercially available overexpressing cell lines was not considered since non-simultaneous OAT expressions might be associated

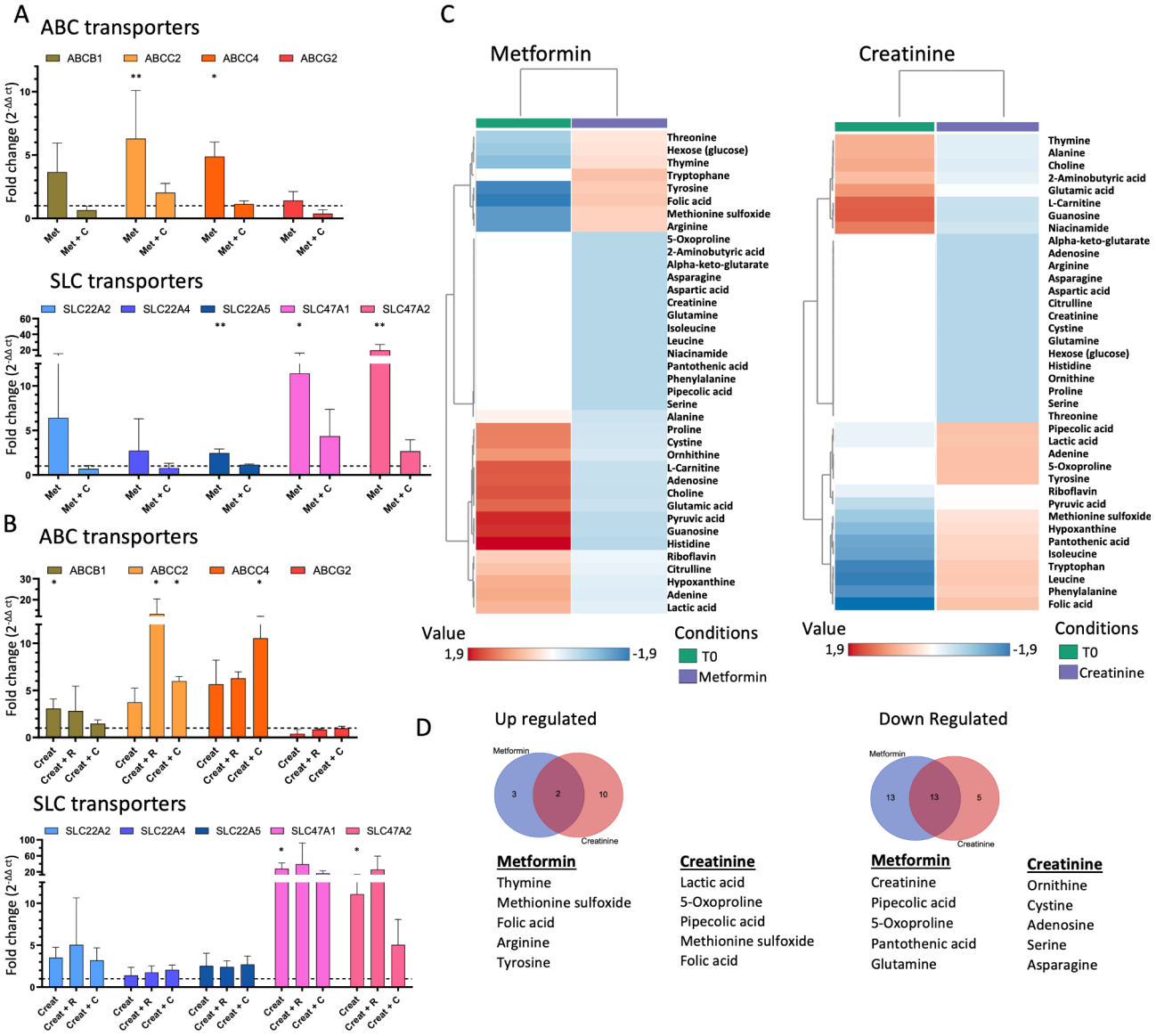

Fig. 3. Metformin and creatinine treatments alter drug transporter transcriptional expression and endogenous metabolite production. Fold changes regarding the relative expression levels of mRNA transporter expressions of RPTEC/TERT1 cell line in dual-channel device under treatment of (**A**) metformin (Met, 100 µM, N = 3), in presence or not of cimetidine (C, 100 µM, N = 3) and (**B**) creatinine (Creat, 10 µM, N = 3) in presence or not of ritonavir (R, 15 µM, N = 3) or cimetidine (C, 100 µM, N = 3). Error bars represent standard deviations. Statistical significance was determined using Kruskal Wallis test, asterisks (*) indicate statistically significant differences with respect to untreated PT-on-chip (N = 5, *p-value < 0.05, **p-value < 0.01, ***p-value < 0.001). (**C**) Heat map of intracellular metabolites altered under metformin (left panel) and creatinine (right panel) treatment. Data were standardized by auto scaling and hierarchically clustered with Ward method and represented by mean of 3 independent replicates. Metabolomic clustering was achieved using the MetaboAnalyst 6.0 Statistical Analysis online tool. (**D**) Venn diagram of shared up regulated and down regulated metabolite under treatment including the top 5 most up and down regulated for each treatment separately.

with an imbalance between influx and efflux transporters owing to OAT substrate overlaps. To date, only a few microfluidic-based in vitro models have been developed to mimic tubular xenobiotic elimination[27,33–35]. However, they have mostly investigated anionic transepithelial transport or consist of more complex systems that are less reproducible and therefore adapt for standard use. It is worth mentioning that the user-dependence of organ-on-chip models is acknowledged as one of the main drawbacks[36]. Noteworthy, a promising human kidney three-dimensional setup has been proposed modelling the proximal tubule architecture, metabolic activity and, the transepithelial transport of anionic probes only (namely PAH and indoxyl sulfate)[37]. Besides, to the best of our knowledge, only one very recent study has reported a two-dimensional PT-on-chip setup

recapitulating the elimination of both anionic and cationic substrates, but using demanding human induced pluripotent stem cells[27].

The influence of different FSSs on drug membrane transporter expression and intracellular metabolism was investigated to determine the optimal parameters for the present model. FSS-dependent profiles regarding mRNA expression and transport functions suggest different responses among pharmacologically relevant drug membrane transporters. However, such a statement must be smoothed because of the discrepancies in transporters' expression profiles between immortalized cell lines and kidney tissues.

Our results are consistent with former investigations supporting that dynamic microfluidic environments improve transporter expression and tubular reabsorption and secretion process[20,38,39]. For instance, flow-induced FSS was shown to increase other transporters such as SGLT1 transporter favoring transepithelial glucose transport in primary human proximal tubular epithelial cells. Likewise, the efflux capacity of ABCB1/P-gp in the presence of FSS was shown to be improved compared to rocker-based perfusion conditions[19]. Noteworthy, several studies employed PT-on-chips to investigate pharmacologically relevant events, mostly from the pharmacodynamics point of view. This is for example the case for the so-called Nephroscreen platform which is a high-throughput PT-on-chip system dedicated to the prediction of xenobiotic-induced nephrotoxicity [34].

The organ-on-chip technology still suffers from a lack of reproducibility and transferability, due to differences in lab practices, as well as to inherent experimental variability (flow, tubing setup).[36,40]. Since 2015, the number of papers published is correlated with that of commercial solutions[26]. It is important to distinguish turnkey systems combining microfluidic platforms and integrated chips[41,42] from adaptative setups including independent microfluidic systems and commercially available chips, tailored to the tissues and objectives. The former limits the integration of additional biological compartments in a physiologically relevant configuration, or accessories such as oxygen sensors or electrodes for barrier integrity measurements. We here propose a robust combination of commercial systems for microfluidic control and microchips, suited to our rather complex double-flow PT model. Lack of reproducibility is also associated with the setup miniaturization as compared with conventional static 2D conditions leading to scalability issues. Therefore, to decipher the effect of FSS, we compared different flow rates (namely 5, 10 and 20 µL/min) with commercial chips exposed to an undetermined FSS in which flow does not apply unidirectionally. Such an undetermined FSS setup was mandatory since static cell culture in miniaturized devices substantially decreased cell viability owing to (i) lack of oxygenation and (ii) toxic imbalance between cell medium nutrients and metabolic waste. Furthermore, we here showed that antiparallel directional flows systematically improved transporter expressions as well as transepithelial transport as compared with rocker-based perfusion. Noteworthy, the choice of flow rate is an important parameter to ensure reproducibility. Unfortunately, in vivo tubular flow rate remains unclear, FSS ranging from 0.3 dyn/cm^2 to 1.6 dyn/cm^2 which was non-compatible with our experimental setup. For instance, cell culture was not possible while applying the maximum flow rate possible (80 µL/min, 0.127 dyn/cm^2) with the Elveflow OB1 MK4 microfluidic system. It is important to note that there is still no consensus for optimal flow rate applied to PT-on-chip systems in the literature adding to the known user- and lab-dependence[36] and aforementioned lack of reproducibility and transferability.

Miniaturization also raises the question about substrate and inhibitor concentrations from conventional in vitro setup to microfluidic chips. This is particularly true to allow comparison with in vivo PK data, for which saturation of the system should be avoided[43,44]. Since the main objective of the present study was to demonstrate the mechanistic relevance of our system to qualitatively model DDIs and DMIs, we here adopted probe concentrations used in the literature [27,45–47]. Although concentrations used in the present studies are higher than expected in an in vivo environment accounting for potential adsorption on-chip and tubing material, the present study paves the way for further investigations to determine not only scaling from in vitro to OoC system experiments but also from OoC to in vivo observation; the latter requiring in silico modelling to the so-called in vitro to in vivo extrapolation[48] (IVIVE) as stressed out pas by Navis et al[43].

With this experimental setup, our objective is to investigate further the underrated transported-mediated interplay between xenobiotics and endogenous metabolites. This new concept, named "remote sensing signaling (RSS) theory", was originally defined as hormone-free inter-organ communication ensuring the homeostasis of small endogenous metabolites[10,49–51]. It has been recently proposed that key pharmacological partners, such as membrane transporters and drug metabolism enzymes, might play a role in the so-called RSS network. Therefore, it has been hypothesized that drug-metabolite interactions, though RSS, may participate in the intra- and inter-individual variabilities of drug pharmacokinetics, efficacy or toxicity. For instance, incorporating uremic solute-mediated OAT1/3 inhibition was shown to improve PBPK prediction of tenofovir renal and systemic disposition[52]. Likewise, it has been shown in vitro that simultaneous exposure of uremic toxins with selected drugs significantly modulates OAT1 transport activity[53] This is in line with recent perspectives which stress out the need to investigate membrane transporter beyond their role in "drug" membrane translocation and in system PK[7]to potentially shift the current PK paradigm by accounting for biological basis of "drug" membrane transporters[10,54].

The present study confirmed membrane transporter competition for creatinine, cimetidine and to a lesser extent ritonavir. Using the same setup, we were able to simultaneously investigate the transcriptomics and metabolomics modifications associated with FSS variations and substrate exposure, as well as transcellular transport. We also showed that xenobiotic exposure may modulate the expression of other transporters, and the intracellular metabolism which may in turn affect local PK (see an example in Fig. 4). Therefore, our system supports the study of disease-like fluid compositions and fluid dynamics, as well as their influence on transporters' function and subsequent local drug PK. Moreover, these results support that mapping metabolite profiles, and interactions involving drug metabolite enzymes and membrane transporters, will improve our understanding of the interplay between RSS and (local) PK. Since they are limited to the OCT2/MATEs transporter pathway,

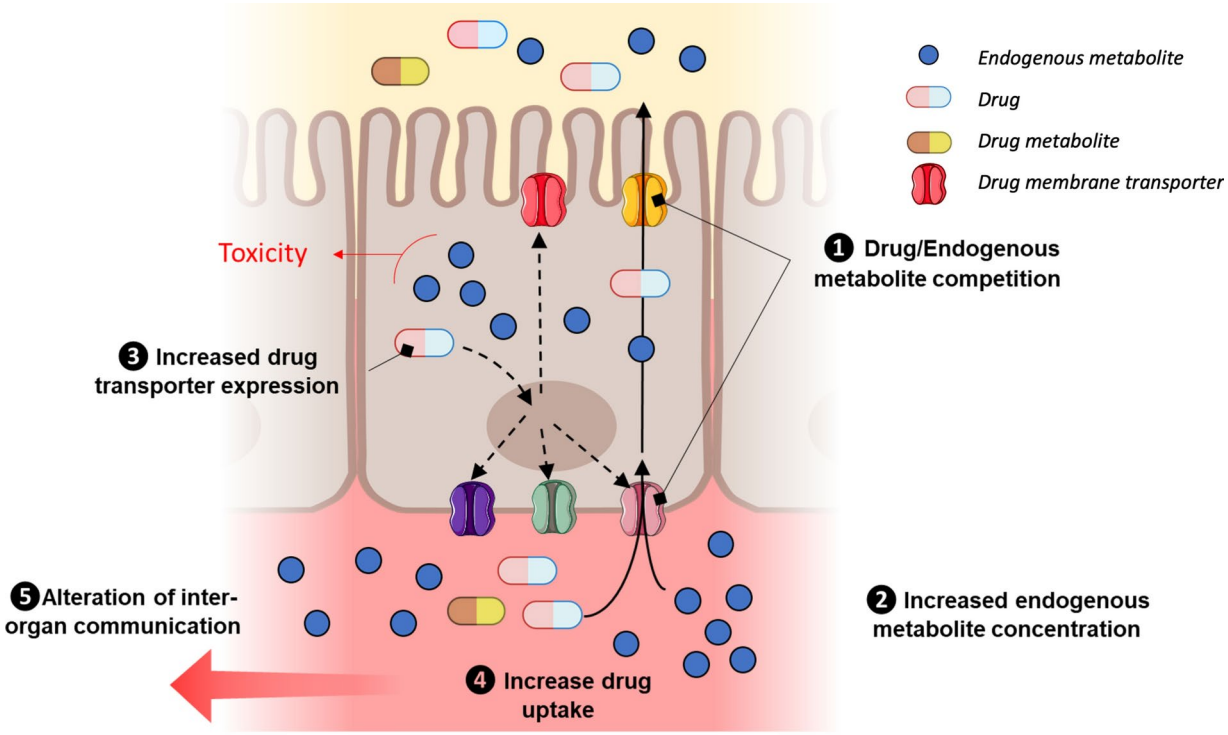

Fig. 4. Prototypical example of transporter-mediated drug-metabolite interplay. (1) Assuming a competition (i) between xenobiotic and endogenous metabolite for influx and efflux transport, this may lead (ii) to increased intracellular concentration of endogenous metabolite and in the systemic circulation. This might be associated with an overexpression of influx and efflux membrane transporter (3) which in turn enhances drug uptake (4) and lowers systemic drug concentration. Additionally, modulation of systemic endogenous metabolite concentration will lead to transporter expression in other tissues owing to a potential alteration of RSS-mediated inter-organ communication (5).

further investigations will be required to extend such knowledge to other renal transporters of clinical and pharmacological importance,[7] as well as to other tissues.

It has been shown that ABC and SLC transporters and drug metabolism enzymes have a distant, coordinated action over the human body, including in key organs of drug PK. For instance, network analyses of the SLC-ABC-DME relationships along the gut-liver-kidney axis confirmed the modulation of intracellular signaling pathways[49,55,56] (*e.g.*, AHR, PXR, HNF1x and HNF4x) in distant organs. By modeling such events using multi-organ-on-chip technology, it may be possible to elucidate shared mechanisms involved in either endogenous metabolite homeostasis or xenobiotic pharmacokinetics, and bridge the gap between local and systemic PK.

Conclusion

We developed a robust and reproducible kidney proximal tubule-on-chip setup able to model physiologically and pharmacologically relevant urinary excretion, which paves the way to decipher the transporter-mediated interplay between endogenous metabolite homeostasis and drug local PK. Despite technical and experimental challenges, connecting standalone organ-on-chip devices or developing multi-organ-on-chip setups in a dynamic microfluidic environment may permit to model and better understand fundamental intracellular mechanisms and local PK events and possibly extend the remote-sensing theory to drug-endogenous metabolites interactions.

Data availability

Data is provided within the manuscript or supplementary information. Original microscopy pictures, raw data for metabolomics and raw datasets used and/or analyzed during the current study available from the corresponding author on reasonable request.

Received: 31 October 2024; Accepted: 6 January 2025
Published online: 20 January 2025

References

1. Turner, R. M., Park, B. K. & Pirmohamed, M. Parsing interindividual drug variability: An emerging role for systems pharmacology. *Wiley Interdiscip. Rev. Syst. Biol. Med.* **7**, 221–241 (2015).
2. Pirmohamed, M. Pharmacogenomics: current status and future perspectives. *Nat. Rev. Genet.* **24**, 350–362 (2023).
3. Giacomini, K.M. et al. Membrane transporters in drug development. *Nat. Rev. Drug. Discov.* **9** 215–236 (2010)

4. Hillgren, K. M. et al. Emerging transporters of clinical importance: An update from the international transporter consortium. *Clin. Pharmacol. Ther.* **94**, 52–63 (2013).
5. Zamek-Gliszczynski, M. J. et al. Transporters in drug development: 2018 itc recommendations for transporters of emerging clinical importance. *Clin. Pharmacol. Ther.* **104**, 890–899 (2018).
6. Zamek-Gliszczynski, M. J. et al. Transporters in drug development: International transporter consortium update on emerging transporters of clinical importance. *Clin. Pharmacol. Ther.* **112**, 485–500 (2022).
7. Galetin, A. et al. Membrane transporters in drug development and as determinants of precision medicine. *Nat. Rev. Drug. Discov.* **23**, 255–280 (2024).
8. Nigam, S. K. What do drug transporters really do?. *Nat. Rev. Drug Discov.* **14**, 29–44 (2015).
9. Wang, K. & Kestenbaum, B. Proximal tubular secretory clearance. *Clin. J. Am. Soc. Nephrol.* **13**, 1291–1296 (2018).
10. Nigam, S. K. & Granados, J. C. A Biological : The remote sensing and signaling theory. *Clin. Pharmacol. Ther.* **112**, 456–460 (2022).
11. Bleasby, K. et al. Expression profiles of 50 xenobiotic transporter genes in humans and pre-clinical species: A resource for investigations into drug disposition. *Xenobiotica* **36**, 963–988 (2006).
12. Jansen, K., Pou Casellas, C., Groenink, L., Wever, K. E. & Masereeuw, R. Humans are animals, but are animals human enough? A systematic review and meta-analysis on interspecies differences in renal drug clearance. *Drug Discov. Today.* **25**, 706–717 (2020).
13. Huang, J. X. et al. Evaluation of biomarkers for in vitro prediction of drug-induced nephrotoxicity: comparison of HK-2, immortalized human proximal tubule epithelial and primary cultures of human proximal tubular cells. *Pharmacol. Res. Perspec.* **3**, e00148 (2015).
14. Bhatia, S. N. & Ingber, D. E. Microfluidic organs-on-chips. *Nat. Biotechnol.* **32**, 760–772 (2014).
15. Low, L. A., Mummery, C., Berridge, B. R., Austin, C. P. & Tagle, D. A. Organs-on-chips: into the next decade. *Nat. Rev. Drug Discov.* **20**, 345–361 (2021).
16. Raghavan, V. & Weisz, O. A. Discerning the role of mechanosensors in regulating proximal tubule function. *Am. J. Physiol-Renal Physiol.* **310**, F1–F5 (2016).
17. Essig, M. & Friedlander, G. A. A. Tubular shear stress and phenotype of renal proximal tubular cells. *J. Am. Soc. Nephrol.* **14**, S33 (2003).
18. Duan, Y., Weinstein, A. M., Weinbaum, S. & Wang, T. Shear stress-induced changes of membrane transporter localization and expression in mouse proximal tubule cells. *Proc. Natl. Acad. Sci. U S A* **107**, 21860–21865 (2010).
19. Jang, K. J. et al. Human kidney proximal tubule-on-a-chip for drug transport and nephrotoxicity assessment. *Integr. Biol. (United Kingdom)* **5**, 1119–1129 (2013).
20. Vriend, J. et al. Flow stimulates drug transport in a human kidney proximal tubule-on-a-chip independent of primary cilia. *Biochim. Biophys. Acta. Gen. Subj.* **1864**, 129433 (2020).
21. Loskill, P., Hardwick, R. N. & Roth, A. Challenging the pipeline. *Stem Cell Rep.* **16**, 2033–2033 (2021).
22. Mastrangeli, M., Millet, S. & van den Eijnden-Van, R. J. Organ-on-chip in development: Towards a roadmap for organs-on-chip. *Altex.* **36**, 650–668 (2019).
23. Morrissey, K. M., Stocker, S. L., Wittwer, M. B., Xu, L. & Giacomini, K. M. Renal Transporters in Drug Development. *Annu. Rev. Pharmacol. Toxicol.* **53**, 503–529 (2013).
24. Kandasamy, K. et al. Prediction of drug-induced nephrotoxicity and injury mechanisms with human induced pluripotent stem cell-derived cells and machine learning methods. *Sci. Rep.* **5**, 12337 (2015).
25. Irvine, A. R., van Berlo, D., Shekhani, R. & Masereeuw, R. A systematic review of *in vitro* models of drug-induced kidney injury. *Curr. Opin. Toxicol.* **27**, 18–26 (2021).
26. Nguyen, V. V. T. et al. A systematic review of kidney-on-a-chip-based models to study human renal (patho-)physiology. *Dis. Model Mech.* **16**, e050113 (2023).
27. Ma, C. et al. Efficient proximal tubule-on-chip model from hiPSC-derived kidney organoids for functional analysis of renal transporters. *iScience* **27**, 110760 (2024).
28. Caetano-Pinto, P. et al. Amplifying the impact of kidney microphysiological systems: predicting renal drug clearance using mechanistic modelling based on reconstructed drug secretion. *ALTEX* **40**, 408–424 (2023).
29. Caetano-Pinto, P. & Stahl, S. H. Renal Organic Anion Transporters 1 and 3 In Vitro: Gone but Not Forgotten. *Int. J. Mol. Sci.* **24**, 15419 (2023).
30. Faucher, Q. et al. Impact of hypoxia and reoxygenation on the extra/intracellular metabolome and on transporter expression in a human kidney proximal tubular cell line. *Metabolomics* **19**, 83 (2023).
31. Caetano-Pinto, P. et al. In Vitro characterization of renal drug transporter activity in kidney cancer. *Int. J. Mol. Sci.* **23**, 10177 (2022).
32. Verhulst, A., Sayer, R., Broe, M. E. D., D'Haese, P. C. & Brown, C. D. A. Human proximal tubular epithelium actively secretes but does not retain rosuvastatin. *Mol. Pharmacol.* **74**, 1084–1091 (2008).
33. Vormann, M. K. et al. Nephrotoxicity and kidney transport assessment on 3D perfused proximal tubules. *AAPS J* **20**, 90 (2018).
34. Vriend, J. et al. Nephroscreen: A robust and versatile renal tubule-on-a-chip platform for nephrotoxicity assessment. *Curr. Opin. Toxicol.* **25**, 42–48 (2021).
35. Vriend, J. et al. Screening of drug-transporter interactions in a 3D microfluidic renal proximal tubule on a chip. *AAPS J* **20**, 87 (2018).
36. Leung, C. M. et al. A guide to the organ-on-a-chip. *Nat. Rev. Methods Primers* **2**, 1–29 (2022).
37. Weber, E. J. et al. Development of a microphysiological model of human kidney proximal tubule function. *Kidney Int.* **90**, 627–637 (2016).
38. Fukuda, Y. et al. Fluid shear stress stimulates MATE2-K expression via Nrf2 pathway activation. *Biochem. Biophys. Res. Commun.* **484**, 358–364 (2017).
39. Ross, E. J. et al. Three dimensional modeling of biologically relevant fluid shear stress in human renal tubule cells mimics in vivo transcriptional profiles. *Sci. Rep.* **11**, 1–14 (2021).
40. Mastrangeli, M. et al. Building blocks for a European Organ-on-Chip roadmap. *ALTEX* **36**, 481–492 (2019).
41. Wheeler, S. E. et al. Spontaneous dormancy of metastatic breast cancer cells in an all human liver microphysiologic system. *Br. J. Cancer* **111**, 2342–2350 (2014).
42. Clark, A. M. et al. A liver microphysiological system of tumor cell dormancy and inflammatory responsiveness is affected by scaffold properties. *Lab. Chip* **17**, 156–168 (2017).
43. Keuper-Navis, M. et al. The application of organ-on-chip models for the prediction of human pharmacokinetic profiles during drug development. *Pharmacol. Res.* **195**, 106853 (2023).
44. Spaggiari, D., Geiser, L., Daali, Y. & Rudaz, S. A cocktail approach for assessing the *in vitro* activity of human cytochrome P450s: An overview of current methodologies. *J. Pharm. Biomed. Anal.* **101**, 221–237 (2014).
45. Lee, J.-B., Kim, H., Kim, S. & Sung, G. Y. Fabrication and evaluation of tubule-on-a-chip with RPTEC/HUVEC co-culture using injection-molded polycarbonate chips. *Micromachines* **13**, 1932 (2022).
46. Mathialagan, S., Rodrigues, A. D. & Feng, B. Evaluation of renal transporter inhibition using creatinine as a substrate in vitro to assess the clinical risk of elevated serum creatinine. *J. Pharm. Sci.* **106**, 2535–2541 (2017).
47. Vidal, F. et al. In vitro cytotoxicity and mitochondrial toxicity of tenofovir alone and in combination with other antiretrovirals in human renal proximal tubule cells. *Antimicrob. Agents Chemother.* **50**, 3824–3832 (2006).

48. Prantil-Baun, R. et al. Physiologically based pharmacokinetic and pharmacodynamic analysis enabled by microfluidically linked organs-on-chips. *Annu. Rev. Pharmacol. Toxicol.* **58**, 37–64 (2018).
49. Jansen, J. et al. Remote sensing and signaling in kidney proximal tubules stimulates gut microbiome-derived organic anion secretion. *Proc. Natl Acad. Sci. U. S. A.* **116**, 16105–16110 (2019).
50. Nigam, S. K. & Granados, J. C. OAT, OATP, and MRP drug transporters and the remote sensing and signaling theory. *Annu. Rev. Pharmacol. Toxicol.* **63**, 637–660 (2023).
51. Granados, J. C. et al. Regulation of human endogenous metabolites by drug transporters and drug metabolizing enzymes: An analysis of targeted SNP-metabolite associations. *Metabolites* **13**, 171–171 (2023).
52. Chang, S.-Y. et al. Incorporating uremic solute-mediated inhibition of OAT1/3 improves PBPK prediction of tenofovir renal and systemic disposition in patients with severe kidney disease. *Pharm. Res.* **40**, 2597–2606 (2023).
53. Mihaila, S. M. et al. Drugs commonly applied to kidney patients may compromise renal tubular uremic toxins excretion. *Toxins* **12**, 391 (2020).
54. Granados, J. C. & Nigam, S. K. Organic anion transporters in remote sensing and organ crosstalk. *Pharm. Ther.* **263**, 108723 (2024).
55. Rosenthal, S. B., Bush, K. T. & Nigam, S. K. A network of SLC and ABC transporter and DME genes involved in remote sensing and signaling in the gut-liver-kidney axis. *Sci. Rep.* **9**, 11879 (2019).
56. Granados, J. C. et al. AHR is a master regulator of diverse pathways in endogenous metabolism. *Sci. Rep.* **12**, 16625 (2022).

Acknowledgements

The authors thank the BISCEm platform (Univ. Limoges, Inserm US042, CNRS UAR 2015, CHU Limoges) for providing access to mass spectrometry and confocal microscopy equipment as well as Claire Carrion and Emilie Pinault for technical support.

Author contributions

All authors contributed significantly to this work. I.P. and N.V. led the investigation, methodology, data curation, formal analysis, and drafting of the original manuscript, with N.V. also providing supervision and validation. Q.F., J.S.B., and P.G. contributed to investigation and methodology, supporting writing and manuscript review. F.L.S. and A.H. added formal analysis and critical manuscript editing. P.M. and F.D.M. were central to conceptualization, funding acquisition, and project administration, with P.M. ensuring resources and validation, and F.D.M. overseeing project supervision and management.

Funding

This work was supported by the French Government's "Plan de relance" (DIGPHAT 22-PESN-0017) and by grants from the French Research Agency (ANR-21-CE18-0030–01., ANR-19-CE17-0008–01) the Inserm and Région Nouvelle Aquitaine (AAP-NA-ESR 2019 VICTOR and 2023 MUSYPHA), and the Horizon Europe Framework Programme (HORIZON) under Marie Skłodowska-Curie grant agreement No. 101107439 (BBB-UT).

Declarations

Competing interests

P.M. reports a relationship with Sandoz France that includes: consulting or advisory and funding grants. P.M. reports a relationship with Chiesi SA France that includes: consulting or advisory and funding grants. Other authors declare that they have no known competing financial interests or personal relationships that could have appeared to influence the work reported in this paper.

Additional information

Supplementary Information The online version contains supplementary material available at https://doi.org/10.1038/s41598-025-85653-4.

Correspondence and requests for materials should be addressed to N.V. or F.D.M.